tvst

DOI: 10.1167/tvst.6.4.12

Article

Retinal Pigment Epithelial Cells are a Potential Reservoir for Ebola Virus in the Human Eye

Justine R. Smith[1,2,3], Shawn Todd[4], Liam M. Ashander[5], Theodosia Charitou[6,7], Yuefang Ma[5], Steven Yeh[8], Ian Crozier[9], Michael Z. Michael[2], Binoy Appukuttan[2,5], Keryn A. Williams[3,10], David J. Lynn[2,6,*], and Glenn A. Marsh[4,*]

[1] Flinders University School of Medicine, Eye & Vision Health, Flinders Medical Centre, Adelaide, Australia
[2] Flinders University School of Medicine, Flinders Centre for Innovation in Cancer, Flinders Medical Centre, Adelaide, Australia
[3] South Australian Health & Medical Research Institute, SAHMRI: Mind & Brain Theme, Adelaide, Australia
[4] Health and Biosecurity, Commonwealth Scientific and Industrial Research Organisation, Geelong, Australia
[5] Flinders University School of Medicine, Eye & Vision Health, Flinders Medical Centre, Adelaide, Australia
[6] South Australian Health & Medical Research Institute, SAHMRI: EMBL Australia group, Infection & Immunity Theme, Adelaide, Australia
[7] Systems Biology Ireland, University College Dublin, UCD Conway Institute, Dublin, Ireland
[8] Departments of Ophthalmology and Pediatrics, Emory University School of Medicine, Atlanta, GA, USA
[9] Infectious Diseases Institute, Mulago Hospital Complex, Kampala, Uganda
[10] Flinders University School of Medicine, Ophthalmology, Flinders Medical Centre, Adelaide, Australia

Correspondence: Justine R. Smith, Eye & Vision Health, Flinders University, Flinders Medical Centre, Room 4E-431, Flinders Drive, Bedford Park, SA 5042, Australia. e-mail: justine.smith@flinders.edu.au

Received: 21 February 2017
Accepted: 19 June 2017
Published: 14 July 2017

Keywords: Ebola virus; human; eye; infection; pigment epithelial cell

Citation: Smith JR, Todd S, Ashander LM, Charitou T, Ma Y, Yeh S, Crozier I, Michael MZ, Appukuttan B, Williams KA, Lynn DJ, Marsh GA. Retinal pigment epithelial cells are a potential reservoir for Ebola virus in the human eye. Trans Vis Sci Tech. 2017; 6(4):12, doi:10.1167/tvst.6.4.12

Purpose: Success of Ebola virus (EBOV) as a human pathogen relates at the molecular level primarily to blockade the host cell type I interferon (IFN) antiviral response. Most individuals who survive Ebola virus disease (EVD) develop a chronic disease syndrome: approximately one-quarter of survivors suffer from uveitis, which has been associated with presence of EBOV within the eye. Clinical observations of post-Ebola uveitis indicate involvement of retinal pigment epithelial cells.

Methods: We inoculated ARPE-19 human retinal pigment epithelial cells with EBOV, and followed course of infection by immunocytochemistry and measurement of titer in culture supernatant. To interrogate transcriptional responses of infected cells, we combined RNA sequencing with in silico pathway, gene ontology, transcription factor binding site, and network analyses. We measured infection-induced changes of selected transcripts by reverse transcription-quantitative polymerase chain reaction.

Results: Human retinal pigment epithelial cells were permissive to infection with EBOV, and supported viral replication and release of virus in high titer. Unexpectedly, 28% of 560 upregulated transcripts in EBOV-infected cells were type I IFN responsive, indicating a robust type I IFN response. Following EBOV infection, cells continued to express multiple immunomodulatory molecules linked to ocular immune privilege.

Conclusions: Human retinal pigment epithelial cells may serve as an intraocular reservoir for EBOV, and the molecular response of infected cells may contribute to the persistence of live EBOV within the human eye.

Translational Relevance: This bedside-to-bench research links ophthalmic findings in survivors of EVD who suffer from uveitis with interactions between retinal pigment epithelial cells and EBOV.

Introduction

Ebola virus disease (EVD) is a severe acute hemorrhagic fever caused by infection with Ebola virus (EBOV).[1] Uveitis – or inflammation inside the eye – is one of the most serious complications of EVD, and it affects a substantial number of survivors.[2] Recent independent surveys conducted at EVD survivor clinics in Sierra Leone[3,4] have con-

firmed uveitis in 18% and 34% of 277 and 166 attendees, respectively. Occurrence of uveitis in two of eight US survivors suggests this risk may be extrapolated beyond West Africa.[5] Inflammation may affect the anterior and/or posterior eye,[3] causing distinct symptoms and complications.[6] Anterior uveitis is often painful, and may lead to cataract or glaucoma. Posterior uveitis causes a range of visual disturbances, and scarring in the macular region of the retina is common. Regardless of the form, post-Ebola uveitis is aggressive: amongst the Sierra Leone cohort of 277 EVD survivor clinic attendees, 75% of individuals with uveitis had vision loss, and 26% were legally blind (Mattia et al. *IOVS* 2017;57: ARVO E-Abstract 4509).

Mechanisms that permit EBOV to persist within the body after recovery from the acute infection must involve host cell-virus interactions that: (1) moderate replication of the virus, and/or (2) limit immune responses to the virus. The eye exhibits immune privilege, which is the ability to limit inflammation that otherwise would damage a tissue, in order to protect a function essential for survival.[7] The monolayers of pigment epithelial cells that line the retina in the posterior eye, and the iris and ciliary body in the anterior eye, are key components of ocular immune privilege.[8] In particular, the ocular pigment epithelial cells are rich sources of membrane-bound ligands and soluble factors that inhibit inflammatory activities of leukocytes.[9–13] By limiting immune responses, however, ocular pigment epithelial cells may promote persistence of microorganisms within the eye.

In clinical reports of a US physician and EVD survivor who suffered severe uveitis associated with intraocular EBOV,[14,15] retinal scars characterized by hypo- and hyperpigmentation indicated involvement of the retinal pigment epithelium. The finding was also common in a cohort of Liberian EVD survivors with uveitis.[16] On the basis of this clinical observation, and the established immunomodulatory role of ocular pigment epithelial cells, we initiated an investigation of post-Ebola uveitis by focusing on infection of human retinal pigment epithelial cells. We examined the susceptibility of ARPE-19 human retinal pigment epithelial cells to infection with EBOV and evaluated the antiviral and immunomodulatory responses of these cells to the infection. Our work represents the first study directed at defining the cellular and molecular mechanisms that allow live EBOV to remain within the human eye.

Methods

Culture of Retinal Pigment Epithelial Cell Line and Ebola Virus

The ARPE-19 human retinal pigment epithelial cell line (American Type Culture Collection [ATCC], Manassas, VA)[17] was cultured in 1:1 Dulbecco's modified Eagle's medium (DMEM):F12 medium (Thermo Fisher Scientific-GIBCO, Grand Island, NY) supplemented with heat-inactivated 10% fetal bovine serum (FBS; GE Healthcare-Hyclone, Logan, UT) at 37°C and 5% CO_2 in air. Phenotype of cells was verified by confirming the presence of 69 retinal pigment epithelial cell signature transcripts, which are expressed by the ARPE-19 cell line,[18] in the RNA sequencing (RNA-seq) transcriptional profile of EBOV- and mock-infected cells (Gene Expression Omnibus [GEO] Accession Number GSE100839). Ebola virus (*Zaire ebolavirus*, EBOV variant Mayinga) was amplified in Vero C1008 cells (European Collection of Authenticated Cell Cultures [ECACC], Salisbury, UK), cultured with DMEM supplemented with 10% FBS at 37°C and 5% CO_2 in air, and titrated by end-point dilution of culture supernatant in fresh Vero C1008 cell monolayers.

Infection of Retinal Pigment Epithelial Cells with Ebola Virus

Confluent monolayers of ARPE-19 cells were inoculated with EBOV at a multiplicity of infection of 5, or mock-infected, in minimum volumes of DMEM:F12 medium with 10% FBS for 30 to 40 minutes, subsequently washed twice with fresh medium, and finally returned to standard volumes of medium, all at 37°C and 5% CO_2 in air. Infected cell monolayers were incubated for up to 72 hours. After predetermined time intervals during this 72-hour period, supernatant was collected and frozen at −80°C, and cells were either fixed in 10% neutral buffered formalin for 48 hours, washed with phosphate buffered saline (PBS), and stored at 4°C for immunocytochemistry, or lysed with TRIzol Reagent (Thermo Fisher Scientific-Invitrogen, Carlsbad, CA) and stored at −80°C ahead of RNA extraction for RNA-seq or reverse transcription (RT)-quantitative polymerase chain reaction (qPCR). All work with live EBOV was conducted under biosafety level 4 conditions, including the use of positive pressure personnel suits with segregated air supply, at the Health and Biosecurity Section of the Commonwealth Scientific

and Industrial Research Organisation (Geelong, Australia).

Immunocytochemistry

Confluent monolayers of fixed EBOV-infected ARPE-19 cells were permeabilized with 0.1% Nonidet P-40 (Sigma-Aldrich, St. Louis, MO) for 10 minutes and blocked with PBS 1% bovine serum albumin (Sigma-Aldrich) for 90 minutes. Cells were incubated overnight at room temperature with rabbit anti-*Ebolavirus* nucleoprotein antiserum,[19] diluted 1:200 in blocking solution. Subsequently, cells were washed three times with PBS with 0.05% Tween 20 (PBS-T), and incubated with Alexa Fluor 488-conjugated goat anti-rabbit secondary antibody (Thermo Fisher Scientific-Molecular Probes, Eugene, OR) at 2 µg/mL in blocking solution for 60 minutes. Finally, monolayers were washed three times with PBS-T, treated with 0.1 µg/mL nM 4′6-diamidino-2-phenylindole-dihydrochloride (Sigma-Aldrich) in PBS for 10 minutes, and washed three times in PBS-T and two times in PBS. Immunolabeled ARPE-19 cells were imaged on the EVOS FL Cell Imaging System (Thermo Fisher Scientific-Invitrogen) at ×10 magnification. Mock-infected monolayers of ARPE-19 cells were immunolabeled and imaged in parallel as control.

Estimation of Viral Titer

Confluent Vero C1008 cell monolayers were inoculated in triplicate with 10-fold serial dilutions of supernatant from EBOV-infected ARPE-19 cells. After 7 days, cells were fixed for 48 hours with 10% neutral buffered formalin and immunolabeled to detect infected cells, following the method described above. The 50% tissue culture infective dose ($TCID_{50}$) was determined by the Reed-Muench method.[20]

Isolation of Total RNA

Total RNA was extracted from TRIzol Reagent-lysed ARPE-19 cells, according to the manufacturer's instructions, and stored at −80°C ahead of use for RNA-seq and RT-qPCR. RNA concentration was determined by spectrophotometry on the Qubit 2.0 Fluorometer (Thermo Fisher Scientific-Invitrogen) for RNA-seq and on the NanoDrop 2000 (Thermo Fisher Scientific, Wilmington, DE) for RT-qPCR. RNA integrity was confirmed on the 2100 Bioanalyzer (Agilent Technologies, Waldbronn, Germany).

RNA Sequencing

RNA extracted from ARPE-19 cells at 24 hours post-inoculation with EBOV or mock-infection was studied by RNA-seq ($n = 3$ monolayers/condition). Total RNA was depleted of ribosomal RNA and converted to cDNA libraries, using the TruSeq Stranded Total RNA kit with Ribo-Zero Gold (Illumina, San Diego, CA), strictly in accordance with the manufacturer's instructions. RNA samples were diluted to 1.3 pM ahead of sequencing on the Illumina NextSeq 500, which was performed with NextSeq 500/550 High Output Kits (Illumina) for 2 × 75 cycles of sequencing. The PhiX Control v3 library (Illumina) was used as a sequencing control.

Processing and Statistical Analysis of RNA Sequencing Data

The quality and number of reads for each sample were assessed with FastQC v0.11.3 (http://www.bioinformatics.babraham.ac.uk/projects/fastqc/). Adaptors were trimmed from reads, and low-quality bases with Phred scores under 28 were trimmed from ends of reads, using Trimgalore v0.4.0 (http://www.bioinformatics.babraham.ac.uk/projects/trim_galore/). Trimmed reads of less than 20 nucleotides were discarded. Reads passing all quality control steps were aligned to the hg38 assembly of the human genome using TopHat v2.1.0,[21] allowing for up to two mismatches. Reads not uniquely aligned to the genome were discarded. HTSeq-count v0.6.0[22] was used in the union model to assign uniquely aligned reads to UCSC hg38-annotated genes. Data were normalized across libraries by the trimmed mean of M-values (TMM) normalization method, implemented in the R v3.2.2 Bioconductor package, EdgeR v3.10.2.[23]

EdgeR was used to generate multidimensional scaling plots, and to identify differentially expressed genes. Genes with at least one count per million in at least three samples were analyzed for evidence of differential expression between EBOV- and mock-infected ARPE-19 cells, using moderated tagwise dispersions. Differentially expressed genes were defined by 2-fold or greater change, and Benjamini and Hochberg corrected P value or false discovery rate (FDR)[24] less than 0.05. Pathway and gene ontology analyses of differentially expressed genes were performed in InnateDB.[25] Interferon (IFN)-regulated genes were identified in Interferome v2.01.[26] A transcription factor binding site analysis was undertaken using the findMotifs.pl program in HOMER

v4.8,[27] with the human hg19 promoter set to identify enriched motifs. InnateDB was used to construct a network of molecular interactions for differentially expressed genes, or products encoded by those genes, and their first neighbor interactors (i.e., gene, RNA, and protein that interact directly with the differentially expressed genes, according to annotation in InnateDB). Redundant edges, self-interactions, and interactions involving promiscuous interactor, ubiquitin C, were removed. The network was visualized using Cytoscape v3.4.0.[28] Contextually relevant hubs, which interacted significantly with differentially expressed nodes, were identified with the Contextual Hub Analysis Tool (CHAT) (http://f1000research.com/articles/5-1745/). The jActiveModules plugin[29] was used to identify high-scoring differentially expressed subnetworks (parameters: 5 modules; overlap threshold of 0.3; search depth of 1). Innate DB was used to investigate whether these subnetworks were enriched in specific pathway components or gene ontology categories.

Reverse Transcription and Quantitative Polymerase Chain Reaction

Reverse transcription was performed using the iScript Reverse Transcription Supermix for RT-qPCR (Bio-Rad, Hercules, CA), with 500 ng of RNA template yielding 20-µL cDNA. Quantitative PCR was performed on the CFX Connect Real-Time PCR Detection System (Bio-Rad) using 2 µL of cDNA diluted up to 1:10, 4 µL of iQ SYBRGreen Supermix (Bio-Rad), 1.5 µL each of 20-µM forward and reverse primers, and 11 µL of nuclease-free water for each reaction. Primer sequences and product sizes for all transcripts are presented in Supplementary Table S1. Amplification consisted of: a precycling hold at 95°C for 5 minutes; 40 cycles of denaturation for 30 seconds at 95°C; annealing for 30 seconds at 60°C; extension for 30 seconds at 72°C; and a post-extension hold at 75°C for 1 second. A melting curve, representing a 1-second hold at every 0.5°C between 70°C and 95°C, was generated to confirm that a single peak was produced for each primer set. Standard curves, produced with serially diluted product, confirmed PCR efficiency of 85% or greater; in the exceptional case of IFN-α1, PCR efficiency was 75%. Size of PCR product was confirmed by electrophoresis on 2% agarose gel. The cycle threshold was measured, with Cq determination mode set to regression. Relative expression was determined using the mathematical model described by Pfaffl,[30] and normalized to three reference genes – β-2-microglobulin (B2M), glyceraldehyde-3-phosphate dehydrogenase (GAPDH), and TATA-binding protein (TBP) – that were stable by the recommended criteria.[31] Relative expression of transcript in EBOV- and mock-infected ARPE-19 cells were compared by two-tailed Student's *t*-test, using GraphPad Prism v6.04 (GraphPad Software, La Jolla, CA).

Results

Human Retinal Pigment Epithelial Cells are Permissive to Infection and Support the Release of Ebola Virus

Susceptibility of human retinal pigment epithelial cells to infection with EBOV was examined by inoculating confluent monolayers of ARPE-19 cells with EBOV, and subsequently immunolabeling fixed cultures for *Ebolavirus* nucleoprotein, and testing culture medium for presence of live virus by $TCID_{50}$, over the course of 72 hours. At 4 hours post-inoculation, EBOV-infected ARPE-19 cells did not label positively for viral nucleoprotein, but by 24 hours and at subsequent 48- and 72-hour time-points, the cytoplasm of infected cells was strongly positive for the protein, in comparison to the cytoplasm of mock-infected cells, which was negative (Fig. 1A). Following a similar time course to intracellular changes, $TCID_{50}$ of supernatant from infected cultures indicated release of EBOV from ARPE-19 cells at high titer from 24 through 72 hours (mean $TCID_{50}$/mL = $3.1 \times 10^6 - 1.3 \times 10^7$) (Fig. 1B). Response of ARPE-19 cells to EBOV infection was verified by measuring significant changes in the expression of selected viral RNA pattern recognition receptors[32,33] and inflammatory molecules between EBOV- and mock-infected cells by RT-qPCR: DEXD/H-box helicase (DDX)58 and IFN induced with helicase C domain (IFIH)1 (Fig. 1C); and tumor necrosis factor (TNF)-α, interleukin (IL)-6, CCL2, CXCL8, and vascular endothelial growth factor (VEGF)A (Fig. 1D), respectively.

Ebola Virus-Infected Human Retinal Pigment Epithelial Cells Generate a Robust Type I Interferon Response

To comprehensively evaluate the human retinal pigment epithelial cell transcriptional response to infection with EBOV, RNA-seq was performed on total RNA extracted from ARPE-19 cell monolayers

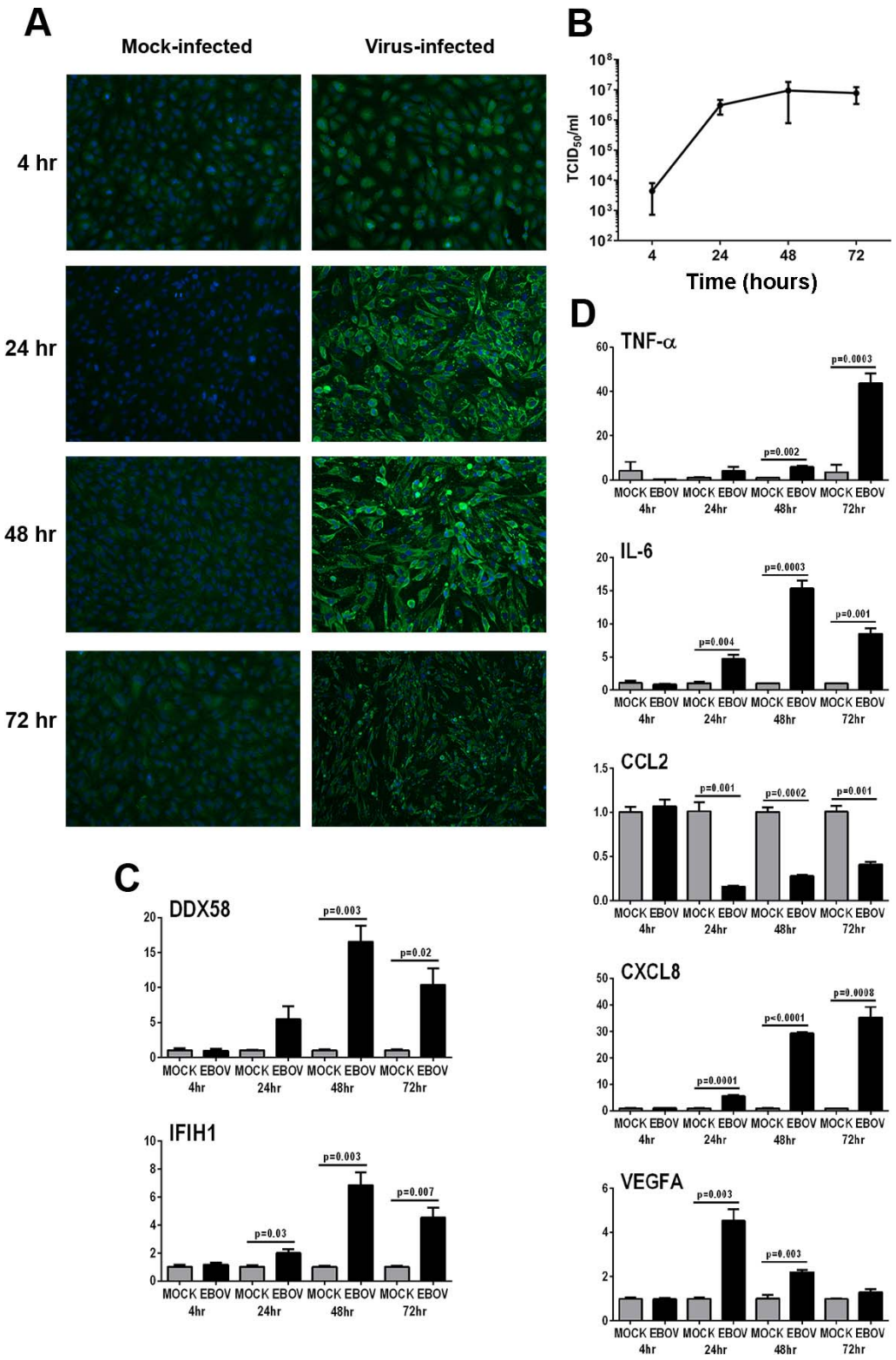

Figure 1. Infection of human retinal pigment epithelial cells with EBOV (multiplicity of infection = 5; evaluated time-points post inoculation = 4, 24, 48, and 72 hours). (A) EBOV-infected and mock-infected ARPE-19 cells immunolabeled to detect *Ebolavirus* nucleoprotein. Alexa Fluor 488 (*green*) with DAPI nuclear counterstain (*blue*). Original magnification: ×10. (B) Graph of $TCID_{50}$ for culture supernatant collected from EBOV-infected ARPE-19 cell monolayers. $n = 3$ cultures/condition. *Dots* represent mean $TCID_{50}$/mL, with *error*

→

←
bars showing SD. (C, D) Graphs showing relative transcript expression for selected viral RNA pattern recognition receptors (C) and inflammatory molecules (D) in EBOV-infected ARPE-19 cells versus mock-infected cells. *Bars* represent mean relative expression, with *error bars* showing SEM. $n = 3$ cultures/condition, with exception of 72-hour mock-infected (2 cultures, pooled, and tested in triplicate). Data were analyzed by two-tailed Student's *t*-test.

24 hours following infection with virus or mock-infection. Across six isolates ($n = 3$ isolates/condition), there were 46.7×10^6 mean paired reads; 40.3×10^6 mean paired reads aligning to the human genome (87%); and 22.2×10^6 mean paired reads aligning unambiguously to annotated genes (55%). Alignment statistics are presented in Supplementary Table S2. Multidimensional scaling analysis demonstrated clear separation of the transcriptomes of ARPE-19 cell monolayers exposed to EBOV versus those of mock-infected cell monolayers (Supplementary Fig. S1). A total of 1060 genes were differentially expressed between ARPE-19 cells infected with EBOV and mock-infected cells; 560 transcripts were significantly increased and 500 transcripts were significantly decreased in EBOV-infected ARPE-19 cells (Supplementary Table S3). Pathway and gene ontology analyses revealed the list of transcripts upregulated in EBOV-infected ARPE-19 cells was enriched for genes annotated in type I IFN signaling, as well as related antiviral responses (Fig. 2; Supplementary Tables S4, S5).

Additional in silico analyses were employed to further interrogate the RNA-seq data set. The Interferome database of IFN-regulated genes[26] identified 155 (28%) of significantly increased transcripts as being type I IFN-responsive (Supplementary Table S6). Transcription factor binding site analysis showed four binding sites to be enriched in the promoter regions of highly expressed genes, including IFN-stimulated response element (ISRE); no binding sites were enriched in genes with low expression (Table 1). System-level network analysis of interactions between differentially expressed genes, or products encoded by those genes, and their first neighbor interactors, yielded a molecular interaction network consisting of 8104 nodes and 20,021 edges (Figs. 3A, 3B). Seven contextual hubs that interacted with differentially expressed genes more frequently than predicted by chance alone included key regulators of the type I IFN response, that is, IFN regulatory factor (IRF)3, IRF9, and signal transducer and activator of transcription (STAT)2 (Table 2). Within the network, one high-scoring subnetwork of upregulated genes (Fig. 3C; Supplementary Fig. S2; 177 nodes and 386 edges) and one high-scoring subnetwork of downregulated genes (Fig. 3D; Supplementary Fig. S3; 241 nodes and 429 edges) were identified; gene ontology indicated the former was significantly enriched in molecules involved in the innate immune response, including IFN-stimulated gene products (FDR: 3.5×10^{-16}), and in the unfolded protein response (FDR: 8.3×10^{-8}), while the latter was significantly enriched in molecules involved in the intrinsic apoptotic pathway (FDR: 5.1×10^{-8}).

Activation of the type I IFN response by EBOV-infected human retinal pigment epithelial cells was confirmed by RT-qPCR of ARPE-19 cell isolates taken at 4, 24, 48, and 72 hours post-inoculation with virus or mock-infection: IFN-β was significantly increased from 24 through 72 hours post inoculation, and 15 selected IFN-stimulated gene products with antiviral activity[34] were significantly increased at one or more time-points from 24 hours (Fig. 4).

Human Retinal Pigment Epithelial Cells Continue to Express Immunomodulatory Molecules Following Infection with Ebola Virus

Human retinal pigment epithelial cells contribute to ocular immune privilege through the constitutive expression of immunomodulatory molecules, including cytokines and other soluble molecules, and membrane-bound ligands.[7] The effect of EBOV on the expression of 10 key immunoregulatory molecules[7–13] by ARPE-19 cells was studied by RT-qPCR on RNA isolates made at 4, 24, 48, and 72 hours post-inoculation with EBOV (Fig. 5). For six molecules, infection with EBOV either had no effect on expression or did not induce sustained changes in expression; these molecules included cytokines: transforming growth factor (TGF)-β2, IL-1 receptor antagonist (IL-1RN), IL-10, and macrophage migration inhibitory factor (MIF); enzyme: prostaglandin E synthase (PTGES) 3, which catalyzes the synthesis of prostaglandin E2; and membrane-bound ligand: Fas ligand (FASLG). Expression of two membrane-bound ligands was significantly increased from 24 hours though 72 hours: programmed death-ligand (PD-L) 1 and PD-L2. Expression of two soluble immunoregulatory factors was significantly decreased from 24 or 48 hours through 72 hours: thrombospondin (TSP)1 and pigment epithelium-derived factor (PEDF).

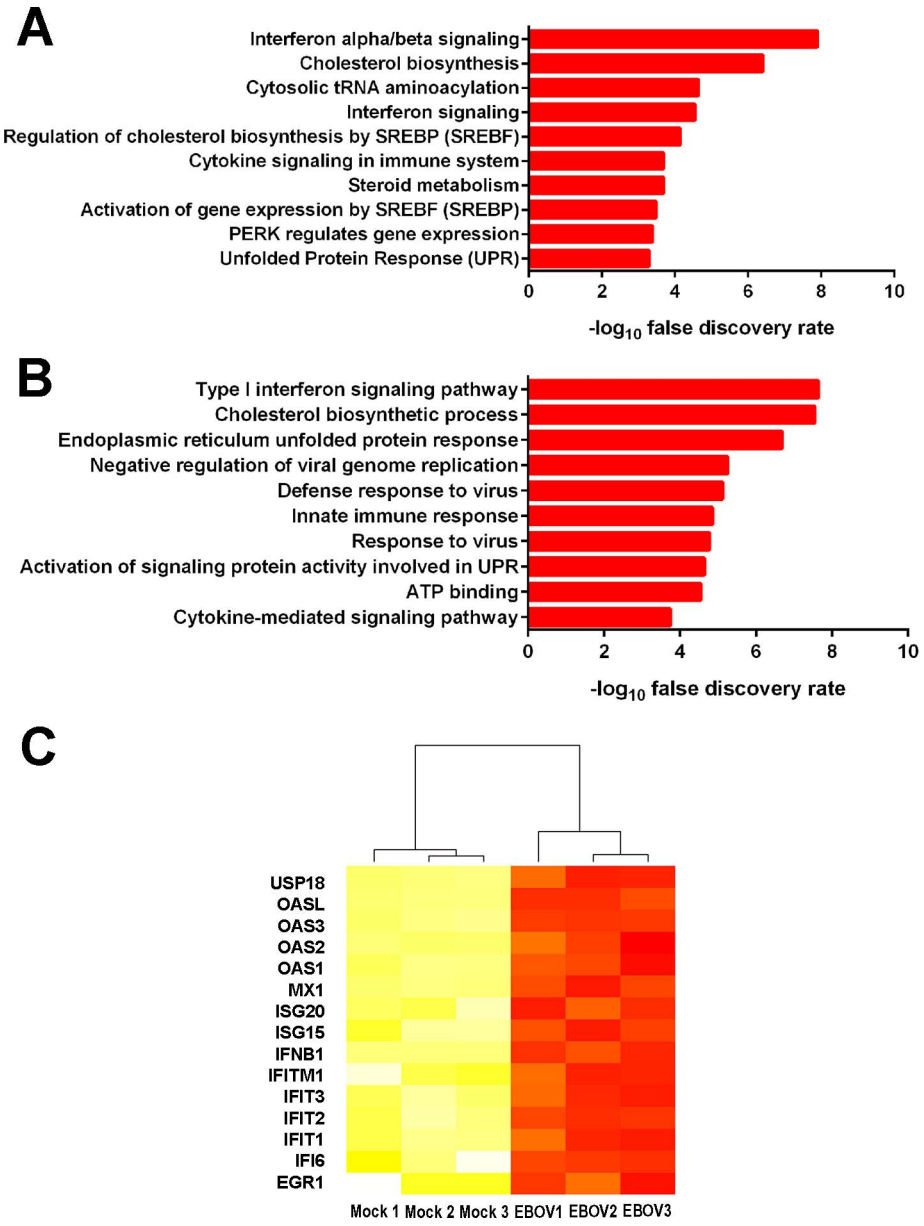

Figure 2. Gene expression changes in human retinal pigment epithelial cells infected with EBOV (multiplicity of infection = 5; evaluated time-point post inoculation = 24 hours) by RNA sequencing. (A, B) Graphs present 10 most highly enriched pathways (A) and gene ontology terms (B) for the 560 gene products that were significantly more highly expressed in EBOV-infected ARPE-19 cells in comparison to mock-infected cells, as annotated in InnateDB.[25] *Horizontal bars* indicate –log10 false discovery rate for each pathway or gene ontology term. (C) Heatmap of normalized counts per million for InnateDB-annotated IFN-regulated genes. Color scale runs from *yellow* to *red*, with *higher intensity red* representing higher counts for each transcript in either the mock-infected or EBOV-infected ARPE-19 cells. $n = 3$ cultures/condition. USP18, ubiquitin specific peptidase 18; OAS, 2′,5′-oligoadenylate synthetase; MX1, MX dynamin-like GTPase 1; ISG, IFN-stimulated gene; IFITM, IFN-induced transmembrane protein; IFIT, IFN-induced protein with tetratricopeptide repeats; IFI6, IFN-α inducible protein 6; EGR1, early growth response 1.

Discussion

Uveitis is a common feature of the post-Ebola syndrome, which affects a majority of individuals who survive EVD.[2] This potentially blinding condition is associated with persistence of live EBOV within the eye.[14] The finding of retinal lesions involving the pigment epithelium prior to the onset of frank inflammation, in the index case of post-Ebola uveitis,[14,15] focused our investigation of disease mechanisms on retinal pigment epithelial cells. We

Table 1. Transcription Factor Binding Sites That Were Enriched in Promoters of Highly Expressed Genes (Target Sequences) in Comparison with All Genes (Background Sequences) in ARPE-19 Human Retinal Pigment Epithelial Cells 24 Hours Following Infection with EBOV

Motif	Consensus Sequence	Number of Target Sequences with Motif (%)	Number of Background Sequences with Motif (%)	False Discovery Rate
CHOP	ATTGCATCAT	20 (4.4)	188 (1.6)	0.034
CEBP:AP1	DRTGTTGCAA	47 (10.3)	680 (5.9)	0.034
HIF-1α	TACGTGCV	44 (9.7)	641 (5.6)	0.036
ISRE	AGTTTCASTTTC	12 (2.6)	93 (0.8)	0.041

CHOP, CCAAT-enhancer-binding protein homologous protein; CEBP, CCAAT-enhancer-binding protein; AP1, activator protein 1; HIF-1α, hypoxia inducible factor 1α.

examined the susceptibility of ARPE-19 human retinal pigment epithelial cells to infection with EBOV – responsible for the 2014 West Africa EVD outbreak – and interrogated the host cell transcriptional response to this infection. Our observations suggest that retinal pigment epithelial cells may provide an intraocular reservoir for EBOV. Replication of EBOV occurs in the cytoplasm of the host cell: immunocytochemical detection of increasing viral antigen within the cytoplasm of EBOV-infected cells indicated retinal pigment epithelial cells were permissive to infection with EBOV. High titer of virus was measured in supernatant harvested from infected cell monolayers (i.e., $TCID_{50}$ reaching over 1×10^6/mL), demonstrating that these cells also supported the release of EBOV, and therefore a productive infection. Network analysis of the ARPE-19 cell transcriptome 24 hours post-infection with EBOV, as determined by RNA-seq, showed intrinsic apoptotic signaling pathways had been downregulated. Infection with Ebola virus may promote or inhibit apoptosis in different cells[35,36]: enhanced retinal pigment epithelial cell survival would be expected to contribute to the EBOV titer within the eye.

In silico pathway, gene ontology, and system-level network comparisons of EBOV-infected and mock-infected ARPE-19 cell transcriptomic profiles all revealed that EBOV-infected human retinal pigment epithelial cells generated a robust type I IFN response. Consistent with these results, 28% of significantly upregulated transcripts were identified as type I IFN-responsive in the Interferome database of IFN-regulated genes.[27] Although the type I IFN response is a critical innate immune defense against viral infection, this result was quite unexpected; EBOV causes severe and accelerated pathology, because it prevents the type I IFN response in other human host cells, including the mononuclear phagocyte populations that are its early targets.[37] The major type I IFNs are IFN-α and IFN-β: IFN-β may be more important for the response to EBOV, because treatment with recombinant IFN-β, but not IFN-α, prolongs survival of infected macaques.[38] Both IFN-α and IFN-β signal via the IFN-α/β receptor, activating Janus kinase-STAT intracellular signaling and inducing multiple IFN-stimulated genes.[34] We verified a strong type I IFN response of EBOV-infected ARPE-19 human retinal pigment epithelial cells using RT-qPCR. Infected cells substantially increased the expression of IFN-β in particular, as well as antiviral restriction factors that are controlled by type I IFNs, including factors that inhibit viral entry (e.g., IFN-induced transmembrane protein family members), intracellular replication of virus (e.g., 2′,5′-oligoadenylate synthetase family members), and viral egress from the cell (e.g., IFN-stimulated gene 15 and bone marrow stromal antigen 2). Because the type I IFN response curtails viral replication, it is possible that the interaction between EBOV and any infected retinal pigment epithelial cell acts to limit viral infection of neighboring cells.

The ability of EBOV to manipulate the host cell type I IFN response resides with structural viral proteins, VP35 and VP24. VP35 reduces synthesis of IFN-α/β by binding viral RNA, sequestering it from pattern recognition receptors – DDX58 and IFIH1 – and partner molecules.[32,33] VP35 also limits IFN-α/β gene expression, by competing for kinases that activate key transcription factors, IRF3 and IRF7,[39] and by increasing IRF3 and IRF7 turnover by SUMOylation.[40] VP24 inhibits transcription of IFN-α/β-stimulated genes by binding the karyopherin proteins responsible for shuttling activated STAT1 to the nucleus.[41] Our results imply that retinal pigment epithelial cells have the capacity to resist molecular evasion strategies effected by VP35 and

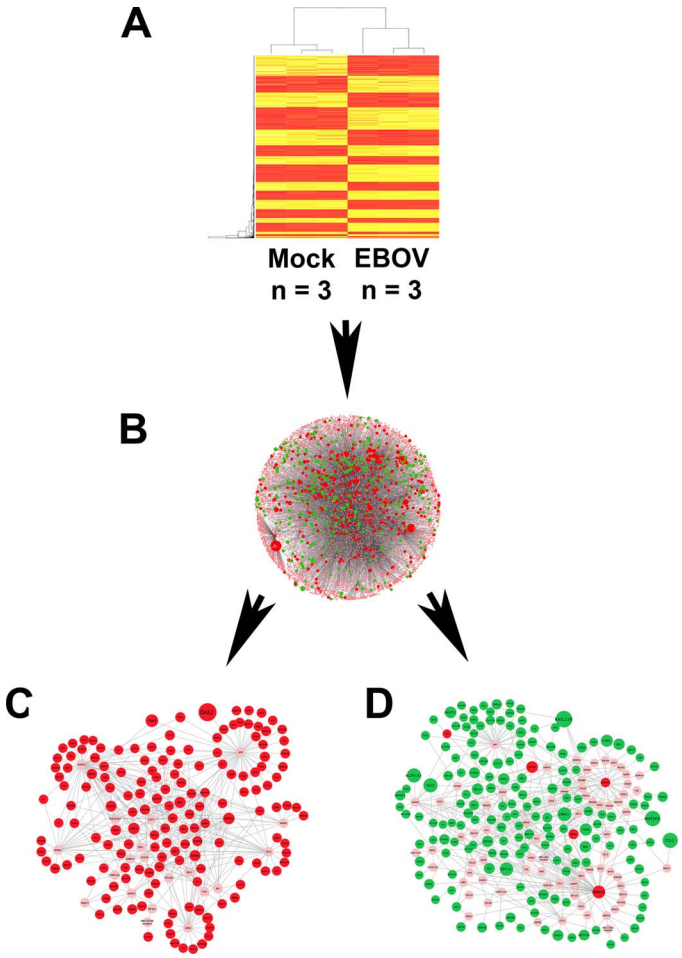

Figure 3. Network analysis of gene expression changes in human retinal pigment epithelial cells infected with EBOV (multiplicity of infection = 5; evaluated time-point post inoculation = 24 hours) by RNA sequencing. (A) Heatmap of the normalized counts per million for genes that were differentially expressed between EBOV-infected or mock-infected ARPE-19 cells. $n = 3$ cultures/condition. Color scale runs from *yellow* to *red*, with *higher intensity red* representing higher counts for each transcript. (B–D) Network schematics representing interactions between differentially expressed genes and their first neighbor interactors, as annotated in InnateDB.[25] *Lines* indicate molecular interactions; *red nodes* indicate upregulated transcripts; *green nodes* indicate downregulated transcripts; *pink nodes* indicate interactors that are not differentially expressed. Node size is proportional to fold-change in gene expression. (C) High-scoring subnetwork enriched in upregulated transcripts. (D) High-scoring subnetwork enriched in downregulated transcripts. Enlarged versions of (C, D) are presented as Supplementary Figs. S2 and S3.

VP24. According to RNA-seq (GEO Accession Number GSE100839), these cells possess the molecular targets of VP35 and VP24 (with the exception of IRF7, which is redundant for signaling where IRF3 is present). While mechanisms of resistance may only be speculated at this time, on that basis, these would potentially include blockade and/or degradation of VP35 and/or VP24, and/or presence of alternate intracellular sensors for EBOV in epithelial cells that trigger type I IFN signaling, perhaps toll-like receptors or nucleotide-binding oligomerization domain-like receptors.[42,43]

Table 2. Contextual Hubs Expressed by ARPE-19 Human Retinal Pigment Epithelial Cells 24 Hours Following Infection with EBOV

Contextual Hubs*	Contextual Neighbors	Total Neighbors	False Discovery Rate
POLR2F	16	142	0.007
ATF4	6	18	0.007
IRF9	7	27	0.007
IRF3	10	64	0.001
RELA	15	153	0.026
BIRC5	4	10	0.041
STAT2	6	29	0.048

POLR2F, RNA polymerase II subunit F; ATF4, activating transcription factor 4; RELA, RELA proto-oncogene, NF-kB subunit; BIRC5, baculoviral IAP repeat containing 5.

* Contextual hubs are molecules that interact with differentially expressed genes (contextual neighbors) more frequently than statistically predicted by chance.

In vitro studies in ARPE-19 cells or other human retinal epithelial cell lines or isolates suggest that this cell population is permissive to infection with a wide range of DNA and RNA viruses, including viruses that do not cause clinical eye disease in an otherwise healthy human: examples include herpes simplex virus, varicella zoster virus, cytomegalovirus (CMV), West Nile virus (WNV), Zika virus, influenza A virus, and vesicular stomatitis virus.[44–51] Multiple reports, describing different aspects of the virus-retinal pigment epithelial cell interaction, reveal infected cells may mount a type I IFN response[46,47,51] and an inflammatory cytokine response.[48,50,51] Of direct relevance to our findings in EBOV-infected retinal pigment epithelial cells, some of these reports further imply the epithelium has a specific molecular phenotype that might promote persistence of live virus within the eye. Cinatl and colleagues[47] observed human retinal pigment cells infected with CMV did not activate the nuclear factor-kappaB (NF-kB)-dependent pathways that promoted viral replication in other cell populations, Separately, the same group[46] found human retinal pigment epithelial cells were capable of IFN-β signaling early in the course of

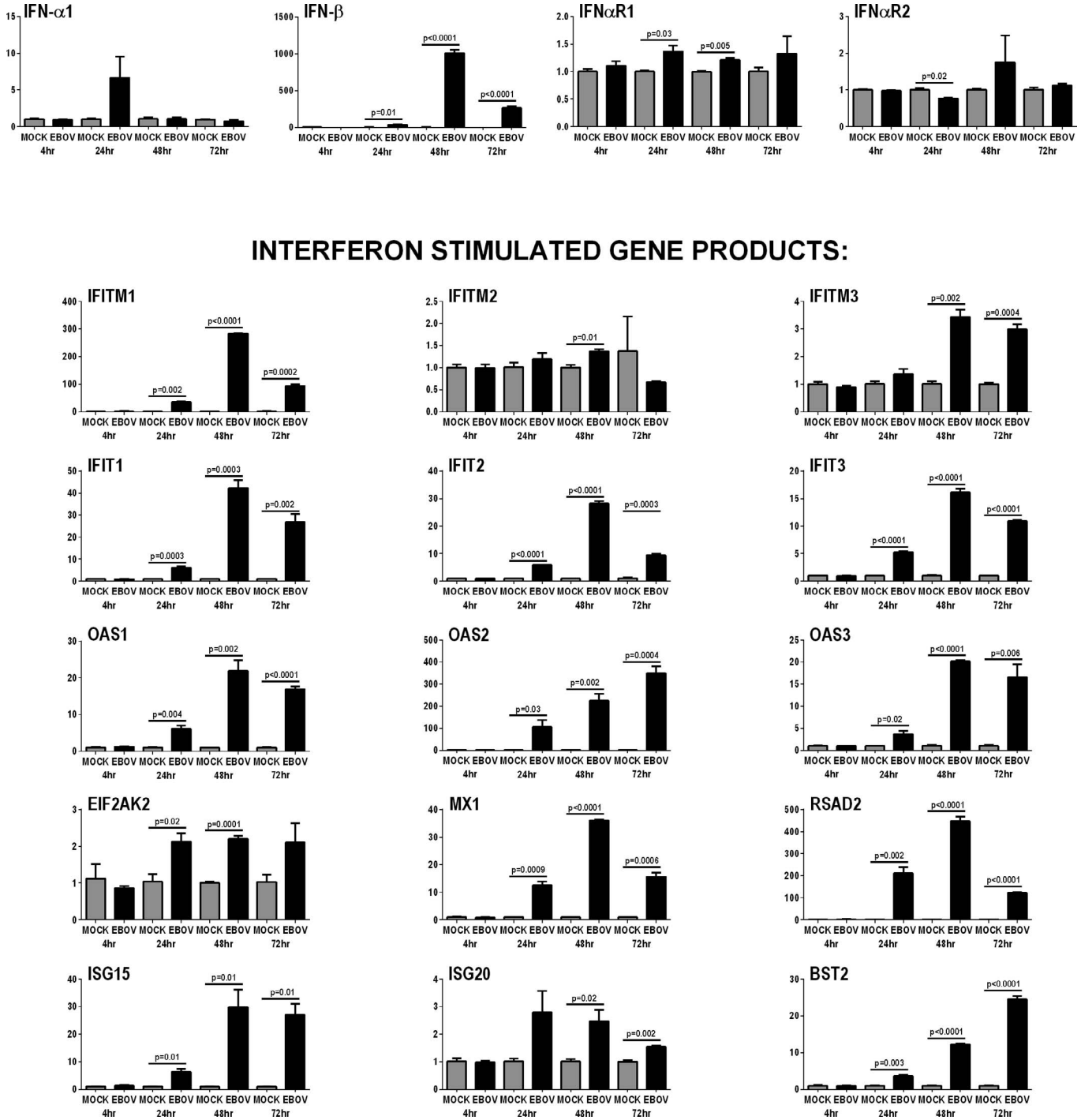

Figure 4. Anti-viral type I IFN response of human retinal pigment epithelial cells infected with EBOV (multiplicity of infection = 5; evaluated time-points post inoculation = 4, 24, 48, and 72 hours). Graphs showing relative transcript expression for IFN-α and IFN-β, plus the IFN receptor subunits, IFN-αR1 and IFN-αR1, and selected IFN-stimulated gene products in EBOV-infected ARPE-19 cells versus mock-infected cells. Reference genes were β-2-microglobulin, glyceraldehyde-3-phosphate dehydrogenase and TATA-binding protein. *Bars* represent mean relative expression, with *error bars* showing SEM. *n* =3 cultures/condition, with exception of 72-hour mock-infected (2 cultures, pooled, and tested in triplicate). Data were analyzed by two-tailed Student's *t*-test. EIF2AK2 = eukaryotic translation initiation factor 2-alpha kinase 2; RSAD2 = radical SAM domain-containing 2; BST2 = bone marrow stromal antigen 2.

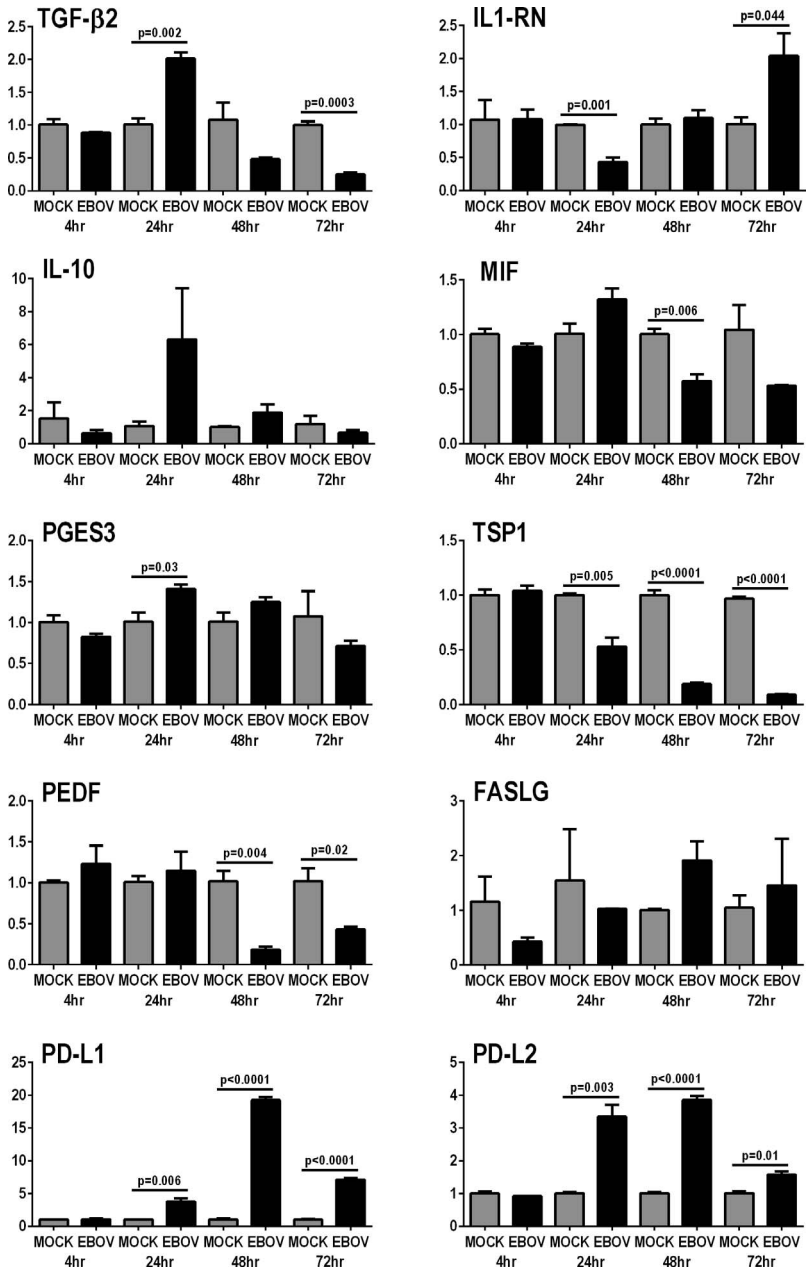

Figure 5. Expression of immunomodulatory molecules by human retinal pigment epithelial cells infected with EBOV (multiplicity of infection = 5; evaluated time-points post inoculation = 4, 24, 48 and 72 hours). Graphs showing relative transcript expression for selected immunomodulatory molecules in EBOV-infected ARPE-19 cells versus mock-infected cells. Reference genes were β-2-microglobulin, glyceraldehyde-3-phosphate dehydrogenase, and TATA-binding protein. *Bars* represent mean relative expression, with *error bars* showing SEM. *n* =3 cultures/condition, with exception of 72 hour mock-infected (2 cultures, pooled, and tested in triplicate). Data were analyzed by two-tailed Student's *t*-test.

WNV infection, despite the presence of viral proteins that limited signaling in other cell types.

Retinal pigment epithelial cells contribute to ocular immune privilege by production of multiple membrane-bound ligands and soluble factors, including cytokines and other proteins, which act to limit inflammation within the eye.[7] While an immunomodulatory environment limits tissue damage during inflammation, it is also conducive to persistence of pathogens. Immune responses to EBOV involve innate and adaptive effector leukocytes[52–55]; restriction of macrophage, natural killer cell, T and B cell activities by ocular pigment epithelial cells have been described.[56–59] Our data suggest that the immuno-

modulatory function of the retinal pigment epithelium is maintained during infection with EBOV, which would limit immune responses against the virus. We did not observe sustained changes in expression of TGF-β2, IL-1RN, IL-10, MIF, PTGES3, and FASLG transcript in EBOV-infected ARPE-19 cells, in comparison with mock-infected control cells. Expression of two soluble immunoregulatory factors – PEDF and TSP1 – decreased following infection, which might promote inflammation; in the mouse eye, PEDF modulates macrophage activation,[10] and TSP1 suppresses bystander T-cell activity.[11] On the other hand, expression of two immunomodulatory membrane-bound ligands – PD-L1 and PD-L2 – was substantially increased after infection. Both PD-L1 and PD-L2 regulate the function of T cells including the $CD8^+$ subset,[60] and increased expression would be expected to reduce an adaptive immune response that might otherwise target EBOV in the eye. Indeed, PD-L1 expressed on ARPE-19 cells limits IFN-γ–induced activation of human peripheral blood T cells.[61] Ocular immune privilege must be overwhelmed for uveitis to be manifest, however, and we observed that EBOV infection led to increased retinal pigment epithelial cell expression of proinflammatory cytokines and chemokines, as well as VEGFA, which is a major enhancer of vascular permeability within the eye.[62]

Our study is the first work to address cellular and molecular mechanisms of EBOV persistence within the human eye. Ebola virus must enter the eye during an acute infection. Our results and previous clinical observations suggest that retinal pigment epithelial cells may serve as one reservoir for EBOV within the eye. We speculate that infected cells activate the type I IFN response, which would limit spread of infection, but that these cells also restrict innate and adaptive immune responses, which otherwise would clear the virus from the eye. Ultimately, infected cells must mount a robust innate immune response that overwhelms ocular immune privilege, leading to clinical uveitis.

A sizeable subset of EVD survivors develop some form of uveitis: certain individuals develop anterior uveitis, while other individuals develop posterior uveitis. Our experiments were conducted with the ARPE-19 cell line, which is a commonly used and well-characterized retinal pigment epithelial cell,[17] although expression levels of certain retinal pigment epithelial cell signature genes are reduced.[18] These cells were originally isolated from the eyes of a 19-year-old donor,[17] but they show changes that suggest an aged or diseased phenotype, including lack of pigmentation and rudimentary intercellular junctional complexes.[63] Observations made in human dendritic cells indicate cells of elderly persons have reduced capacity to mount a type I IFN responses,[64] suggesting the antiviral response to EBOV in the eye may be more intense than is observed in ARPE-19 cells. To dissect interindividual differences in susceptibility to uveitis and preferential localization to the anterior versus posterior eye, evaluation of gene expression following infection of multiple primary human ocular pigment epithelial cell isolates from iris (of the anterior eye) and retina (of the posterior eye) may be highly informative. Published protocols for the isolation and culture of human iris and retinal pigment epithelial cells yield cells that retain the in vivo phenotype at early passage.[65,66] Comparisons of host cell responses to EBOV versus Reston virus, which is pathogenic in nonhuman primates, but not humans,[67] as well as comparisons of responses to EBOV and other viruses that are associated with uveitis, are also likely to provide additional insights into the pathogenesis of post-Ebola uveitis.

Uveitis is arguably the most serious medical complication for individuals who survive EVD, related to the ability of EBOV to persist within the eye following recovery from EVD. Working with live EBOV and the ARPE-19 human ocular pigment epithelial cell line, we have showed that human retinal pigment epithelial cells support the replication of EBOV, and importantly, release EBOV in high titer. Using RNA-seq, we have demonstrated the host cell response to infection involves induction of a robust type I IFN response and maintenance of an immunomodulatory profile. Our findings suggest the interaction between retinal pigment epithelial cells and EBOV may contribute to a microenvironment that allows live virus to remain inside the human eye. These observations may have broad implications for the long-term persistence of EBOV at other body locations.

Acknowledgments

The authors thank Renee Smith and Letitia Pimlott of the Flinders Genomics Facility, and Mark van der Hoek of the South Australian Health & Medical Research Institute David Gunn Genomics Facility for next-generation sequencing services.

Supported by grants from Australian Research

Council (JRS; Future Fellowship 130101648); Flinders University Faculty of Medicine, Nursing & Health Sciences (JRS; Establishment Grant); Teagasc (TC; Walsh Fellowship); Alcon Research Institute (SY; Young Investigator Grant); Research to Prevent Blindness (Unrestricted Grant to Department of Ophthalmology, Emory University School of Medicine); National Health & Medical Research Council Australia (KAW; Principal Research Fellowship 1002044); and EMBL Australia (DJL; Group Leader Award).

Disclosure: **J.R. Smith**, None; **S. Todd**, None; **L.M. Ashander**, None; **T. Charitou**, None; **Y. Ma**, None; **S. Yeh**, None; **I. Crozier**, None; **M.Z. Michael**, None; **B. Appukuttan**, None; **K.A. Williams**, None; **D.J. Lynn**, None; **G.A. Marsh**, None.

*DJ Lynn and GA Marsh contributed equally to this work and share senior authorship of this manuscript.

References

1. Feldmann H, Geisbert TW. Ebola haemorrhagic fever. *Lancet*. 2011;377:849–862.
2. Hunt L, Knott V. Serious and common sequelae after Ebola virus infection. *Lancet Infect Dis*. 2016;16:270–271.
3. Mattia JG, Vandy MJ, Chang JC, et al. Early clinical sequelae of Ebola virus disease in Sierra Leone: a cross-sectional study. *Lancet Infect Dis*. 2016;16:331–338.
4. Tiffany A, Vetter P, Mattia J, et al. Ebola virus disease complications as experienced by survivors in Sierra Leone. *Clin Infect Dis*. 2016;62:1360–1366.
5. Epstein L, Wong KK, Kallen AJ, Uyeki TM. Post-Ebola signs and symptoms in U.S. survivors. *New Engl J Med*. 2015;373:2484–2486.
6. de Smet MD, Taylor SR, Bodaghi B, et al. Understanding uveitis: the impact of research on visual outcomes. *Prog Retin Eye Res*. 2011;30:452–470.
7. Streilein JW. Ocular immune privilege: therapeutic opportunities from an experiment of nature. *Nat Rev Immunol*. 2003;3:879–889.
8. Mochizuki M, Sugita S, Kamoi K. Immunological homeostasis of the eye. *Prog Retin Eye Res*. 2013;33:10–27.
9. Jorgensen A, Wiencke AK, la Cour M, et al. Human retinal pigment epithelial cell-induced apoptosis in activated T cells. *Invest Ophthalmol Vis Sci*. 1998;39:1590–1599.
10. Zamiri P, Masli S, Streilein JW, Taylor AW. Pigment epithelial growth factor suppresses inflammation by modulating macrophage activation. *Invest Ophthalmol Vis Sci*. 2006;47:3912–3918.
11. Futagami Y, Sugita S, Vega J, et al. Role of thrombospondin-1 in T cell response to ocular pigment epithelial cells. *J Immunol*. 2007;178:6994–7005.
12. Horie S, Sugita S, Futagami Y, et al. Human iris pigment epithelium suppresses activation of bystander T cells via TGFbeta-TGFbeta receptor interaction. *Exp Eye Res*. 2009;88:1033–1042.
13. Sugita S, Usui Y, Horie S, et al. T-cell suppression by programmed cell death 1 ligand 1 on retinal pigment epithelium during inflammatory conditions. *Invest Ophthalmol Vis Sci*. 2009;50:2862–2870.
14. Varkey JB, Shantha JG, Crozier I, et al. Persistence of Ebola virus in ocular fluid during convalescence. *New Engl J Med*. 2015;372:2423–2427.
15. Shantha JG, Crozier I, Varkey JB, et al. Long-term management of panuveitis and iris heterochromia in an Ebola survivor. *Ophthalmology*. 2016;123:2626–2628.
16. Shantha JG, Crozier I, Hayek BR, et al. Ophthalmic manifestations and causes of vision impairment in Ebola virus disease survivors in Monrovia, Liberia. *Ophthalmology*. 2017;124:170–177.
17. Dunn KC, Aotaki-Keen AE, Putkey FR, Hjelmeland LM. ARPE-19, a human retinal pigment epithelial cell line with differentiated properties. *Exp Eye Res*. 1996;62:155–169.
18. Strunnikova NV, Maminishkis A, Barb JJ, et al. Transcriptome analysis and molecular signature of human retinal pigment epithelium. *Hum Mol Genet*. 2010;19:2468–2486.
19. Marsh GA, Haining J, Robinson R, et al. Ebola Reston virus infection of pigs: clinical significance and transmission potential. *J Infect Dis*. 2011;204:S804–S809.
20. Reed LJ, Muench LH. A simple method of estimating fifty percent endpoints. *Am J Hyg*. 1938;27:493–497.
21. Kim D, Pertea G, Trapnell C, Pimentel H, Kelley R, Salzberg SL. TopHat2: accurate alignment of transcriptomes in the presence of insertions, deletions and gene fusions. *Genome Biol*. 2013;14:R36.

22. Anders S, Pyl PT, Huber W. HTSeq–a Python framework to work with high-throughput sequencing data. *Bioinformatics*. 2015;31:166–169.
23. Robinson MD, McCarthy DJ, Smyth GK. edgeR: a Bioconductor package for differential expression analysis of digital gene expression data. *Bioinformatics*. 2010;26:139–140.
24. Benjamini YHY. Controlling the false discovery rate: a practical and powerful approach to multiple testing. *J R Stat Soc B*. 1995;57:289–300.
25. Lynn DJ, Winsor GL, Chan C, et al. InnateDB: facilitating systems-level analyses of the mammalian innate immune response. *Mol Syst Biol*. 2008; 4:218.
26. Rusinova I, Forster S, Yu S, et al. Interferome v2.0: an updated database of annotated interferon-regulated genes. *Nucleic Acids Res*. 2013;41: D1040–1046.
27. Heinz S, Benner C, Spann N, et al. Simple combinations of lineage-determining transcription factors prime cis-regulatory elements required for macrophage and B cell identities. *Mol Cell*. 2010;38:576–589.
28. Shannon P, Markiel A, Ozier O, et al. Cytoscape: a software environment for integrated models of biomolecular interaction networks. *Genome Res*. 2003;13:2498–2504.
29. Ideker T, Ozier O, Schwikowski B, Siegel AF. Discovering regulatory and signalling circuits in molecular interaction networks. *Bioinformatics*. 2002;18:S233–S240.
30. Pfaffl MW. A new mathematical model for relative quantification in real-time RT-PCR. *Nucleic Acids Res*. 2001;29:e45.
31. Hellemans J, Mortier G, De Paepe A, Speleman F, Vandesompele J. qBase relative quantification framework and software for management and automated analysis of real-time quantitative PCR data. *Genome Biol*. 2007;8:R19.
32. Cardenas WB, Loo YM, Gale M Jr, et al. Ebola virus VP35 protein binds double-stranded RNA and inhibits alpha/beta interferon production induced by RIG-I signaling. *J Virol*. 2006;80: 5168–5178.
33. Luthra P, Ramanan P, Mire CE, et al. Mutual antagonism between the Ebola virus VP35 protein and the RIG-I activator PACT determines infection outcome. *Cell Host Microbe*. 2013;14:74–84.
34. McNab F, Mayer-Barber K, Sher A, Wack A, O'Garra A. Type I interferons in infectious disease. *Nat Rev Immunol*. 2015;15:87–103.
35. Bradfute SB, Swanson PE, Smith MA, et al. Mechanisms and consequences of ebolavirus-induced lymphocyte apoptosis. *J Immunol*. 2010; 184:327–335.
36. Noyori O, Nakayama E, Maruyama J, Yoshida R, Takada A. Suppression of Fas-mediated apoptosis via steric shielding by filovirus glycoproteins. *Biochem Biophys Res Commun*. 2013; 441:994–998.
37. Edwards MR, Liu G, Mire CE, et al. Differential regulation of interferon responses by Ebola and Marburg virus VP35 proteins. *Cell Rep*. 2016;14: 1632–1640.
38. Smith LM, Hensley LE, Geisbert TW, et al. Interferon-beta therapy prolongs survival in rhesus macaque models of Ebola and Marburg hemorrhagic fever. *J Infect Dis*. 2013;208:310–318.
39. Prins KC, Cardenas WB, Basler CF. Ebola virus protein VP35 impairs the function of interferon regulatory factor-activating kinases IKKepsilon and TBK-1. *J Virol*. 2009;83:3069–3077.
40. Chang TH, Kubota T, Matsuoka M, et al. Ebola Zaire virus blocks type I interferon production by exploiting the host SUMO modification machinery. *PLoS Pathog*. 2009;5:e1000493.
41. Reid SP, Valmas C, Martinez O, Sanchez FM, Basler CF. Ebola virus VP24 proteins inhibit the interaction of NPI-1 subfamily karyopherin alpha proteins with activated STAT1. *J Virol*. 2007;81: 13469–13477.
42. Leung LW, Park MS, Martinez O, Valmas C, Lopez CB, Basler CF. Ebolavirus VP35 suppresses IFN production from conventional but not plasmacytoid dendritic cells. *Immunol Cell Biol*. 2011;89:792–802.
43. Jensen S, Thomsen AR. Sensing of RNA viruses: a review of innate immune receptors involved in recognizing RNA virus invasion. *J Virol*. 2012;86: 2900–2910.
44. Arao Y, Ando Y, Narita M, Kurata T. Unexpected correlation in the sensitivity of 19 herpes simplex virus strains to types I and II interferons. *J Interferon Cytokine Res*. 1997;17:537–541.
45. Cinatl J, Jr., Margraf S, Vogel JU, Scholz M, Cinatl J, Doerr HW. Human cytomegalovirus circumvents NF-kappa B dependence in retinal pigment epithelial cells. *J Immunol*. 2001;167: 1900–1908.
46. Cinatl J, Jr., Michaelis M, Fleckenstein C, et al. West Nile virus infection induces interferon signalling in human retinal pigment epithelial cells. *Invest Ophthalmol Vis Sci*. 2006;47:645–651.
47. Hooks JJ, Nagineni CN, Hooper LC, Hayashi K, Detrick B. IFN-beta provides immuno-protection in the retina by inhibiting ICAM-1 and CXCL9

in retinal pigment epithelial cells. *J Immunol*. 2008;180:3789–3796.
48. Michaelis M, Geiler J, Klassert D, Doerr HW, Cinatl J Jr. Infection of human retinal pigment epithelial cells with influenza A viruses. *Invest Ophthalmol Vis Sci*. 2009;50:5419–5425.
49. Milikan JC, Baarsma GS, Kuijpers RW, Osterhaus AD, Verjans GM. Human ocular-derived virus-specific CD4+ T cells control varicella zoster virus replication in human retinal pigment epithelial cells. *Invest Ophthalmol Vis Sci*. 2009; 50:743–751.
50. Momma Y, Nagineni CN, Chin MS, Srinivasan K, Detrick B, Hooks JJ. Differential expression of chemokines by human retinal pigment epithelial cells infected with cytomegalovirus. *Invest Ophthalmol Vis Sci*. 2003;44:2026–2033.
51. Singh PK, Guest JM, Kanwar M, et al. Zika virus infects cells lining the blood–retinal barrier and causes chorioretinal atrophy in mouse eyes. *JCI Insight*. 2017;2:e92340.
52. Sanchez A, Lukwiya M, Bausch D, et al. Analysis of human peripheral blood samples from fatal and nonfatal cases of Ebola (Sudan) hemorrhagic fever: cellular responses, virus load, and nitric oxide levels. *J Virol*. 2004;78:10370–10377.
53. Wauquier N, Becquart P, Padilla C, Baize S, Leroy EM. Human fatal zaire ebola virus infection is associated with an aberrant innate immunity and with massive lymphocyte apoptosis. *PLoS Negl Trop Dis*. 2010;4:e837.
54. McElroy AK, Akondy RS, Davis CW, et al. Human Ebola virus infection results in substantial immune activation. *Proc Natl Acad Sci U S A*. 2015;112:4719–4724.
55. Messaoudi I, Amarasinghe GK, Basler CF. Filovirus pathogenesis and immune evasion: insights from Ebola virus and Marburg virus. *Nat Rev Microbiol*. 2015;13:663–676.
56. Hattori T, Kezuka T, Usui Y, et al. Human iris pigment epithelial cells suppress T-cell activation via direct cell contact. *Exp Eye Res*. 2009;89:358–364.
57. Sugita S, Horie S, Yamada Y, Mochizuki M. Inhibition of B-cell activation by retinal pigment epithelium. *Invest Ophthalmol Vis Sci*. 2010;51: 5783–5788.
58. Zamiri P, Sugita S, Streilein JW. Immunosuppressive properties of the pigmented epithelial cells and the subretinal space. *Chem Immunol Allergy*. 2007;92:86–93.
59. Sugita S. Role of ocular pigment epithelial cells in immune privilege. *Arch Immunol Ther Exp (Warsz)*. 2009;57:263–268.
60. Riella LV, Paterson AM, Sharpe AH, Chandraker A. Role of the PD-1 pathway in the immune response. *Am J Transplant*. 2012;12: 2575–2587.
61. Yang W, Li H, Chen PW, et al. PD-L1 expression on human ocular cells and its possible role in regulating immune-mediated ocular inflammation. *Invest Ophthalmol Vis Sci*. 2009;50:273–280.
62. Miller JW, Le Couter J, Strauss EC, Ferrara N. Vascular endothelial growth factor a in intraocular vascular disease. *Ophthalmology*. 2013;120: 106–114.
63. Ablonczy Z, Dahrouj M, Tang PH, et al. Human retinal pigment epithelium cells as functional models for the RPE in vivo. *Invest Ophthalmol Vis Sci*. 2011;52:8614–8620.
64. Agrawal A. Mechanisms and implications of age-associated impaired innate interferon secretion by dendritic cells: a mini-review. *Gerontology*. 2013; 59:421–426.
65. Hu DN, Ritch R, McCormick SA, Pelton-Henrion K. Isolation and cultivation of human iris pigment epithelium. *Invest Ophthalmol Vis Sci*. 1992;33:2443–2453.
66. Blenkinsop TA, Saini JS, Maminishkis A, et al. Human adult retinal pigment epithelial stem cell-derived RPE monolayers exhibit key physiological characteristics of native tissue. *Invest Ophthalmol Vis Sci*. 2015;56:7085–7099.
67. Martines RB, Ng DL, Greer PW, Rollin PE, Zaki SR. Tissue and cellular tropism, pathology and pathogenesis of Ebola and Marburg viruses. *J Pathol*. 2015;235:153–174.